

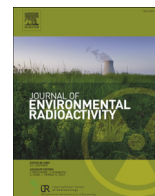
日本原子力研究開発機構機関リポジトリ
Japan Atomic Energy Agency Institutional Repository

Title	The Transfer of radiocesium from the bark to the stemflow of chestnut trees (<i>Castanea crenata</i>) contaminated by radionuclides from the Fukushima Dai-ichi Nuclear Power Plant accident
Author(s)	Sasaki Yoshito, Abe Hironobu, Mitachi Katsuaki, Watanabe Takayoshi, Ishii Yasuo, Niizato Tadafumi
Citation	Journal of Environmental Radioactivity,161,p.58-65
Text Version	Publisher's Version
URL	https://jopss.jaea.go.jp/search/servlet/search?5050807
DOI	https://doi.org/10.1016/j.jenvrad.2015.12.001
Right	© 2015 The Authors. Published by Elsevier Ltd.This is an open access article under the CC BY-NC-ND license (http://creativecommons.org/licenses/by-nc-nd/4.0/)



Contents lists available at ScienceDirect

Journal of Environmental Radioactivity

journal homepage: www.elsevier.com/locate/jenvrad

The transfer of radiocesium from the bark to the stemflow of chestnut trees (*Castanea crenata*) contaminated by radionuclides from the Fukushima Dai-ichi nuclear power plant accident

Yoshito Sasaki*, Hironobu Abe, Katsuaki Mitachi, Takayoshi Watanabe, Yasuo Ishii, Tadafumi Niizato

Fukushima Environmental Safety Center, Japan Atomic Energy Agency, Sahei 8F, 1-29, Okitama-cho, Fukushima-shi, Fukushima 960-8034 Japan

ARTICLE INFO

Article history:

Received 23 June 2015

Received in revised form

30 November 2015

Accepted 1 December 2015

Available online xxx

Keywords:

Fukushima Daiichi

Cesium

Deciduous broadleaf tree

Stemflow

Chestnut

ABSTRACT

We report on the behavior of radiocesium in tree bark and its transfer into the stemflows of chestnut trees in a forest in the Fukushima Prefecture, Japan. In stems that were present at the time of the accident, the radiocesium concentration of the bark was found to be approximately 10 times that of the wood. The average ^{137}Cs concentration of the dissolved fraction ($<0.45\ \mu\text{m}$) in the stemflow was measured to be around 10 Bq/L. The ^{137}Cs concentration ratio [present at the time of the accident (Bq/kg) in the bark/the dissolved fraction in the stemflow (Bq/L)] was approximately 10^3 . A strong positive correlation was observed between the radiocesium concentration and the electrical conductivity of the dissolved fraction of the stemflow; this result suggests that radiocesium and electrolytes have the same elution mechanism from the tree. The size fractionation analysis of the $<0.45\ \mu\text{m}$ fraction through ultrafiltration revealed that the radiocesium was present as an almost dissolved species. Some of the particles in the particulate fraction ($>0.45\ \mu\text{m}$) of the stemflow were strongly adsorbed radiocesium.

© 2015 The Authors. Published by Elsevier Ltd. This is an open access article under the CC BY-NC-ND license (<http://creativecommons.org/licenses/by-nc-nd/4.0/>)

1. Introduction

Numerous radionuclides were released into the environment as a result of the accident at the Fukushima Dai-ichi nuclear power plant (FDNPP) of the Tokyo Electric Power Company, which occurred as a result of the Great East Japan Earthquake on March 11, 2011 (Chino et al., 2011). Radionuclides with short half-lives, such as ^{131}I (8.04 d half-life), decayed in a few months; however, many of those with relatively long half-lives, such as ^{134}Cs (2.06 y half-life) and ^{137}Cs (30.2 y half-life), are still present in the environment. Radiocesium falls to the ground as particulate matter containing Fe, Zn, and Cs (Adachi et al., 2013) or aerosols (Kaneyasu et al., 2012). Because the leaves of deciduous broad-leaved trees had already fallen at the time of the accident, radiocesium from the FDNPP contaminated the exposed stems and branches. Potassium and cesium are congeners, i.e., they have similar behavior, and these elements are easily incorporated into plants. Radiocesium contamination of the wood in these areas has led to restrictions on

the usage of the wood and serious damage to the forestry industry. The possibility of the transmission of radiocesium from the barks to the interiors of trees has been reported in the Fukushima Prefecture (Mahara et al., 2014). Stemflow is the leaching of radiocesium deposited on the bark by rain and represents another radiocesium transfer pathway (Kato et al., 2012; Teramaga et al., 2014; Loffredo et al., 2014). The annual rainfall values for the entire Fukushima Prefecture and for Kawamata town (the study site) are 1166 mm and 1368 mm, respectively (Japan Meteorological Agency, 2014). In the case of Chernobyl, the annual total rainfall values of Kiev (approximately 115 km to the south of the Chernobyl nuclear power plant [CNPP]) and Minsk (approximately 330 km northwest of the CNPP) are 608 mm and 690 mm, respectively (Chronological Scientific Tables, 2014). On the basis of these rainfall values, the influence of radiocesium leaching by rainfall around the FDNPP would be expected to be larger than that in the area surrounding Chernobyl. Details of the transfer of radiocesium from the trees to the ground in the forest remain unknown.

This study aims to elucidate the transition mechanism of radiocesium to stemflow from bark that has been contaminated with radiocesium in deciduous broad-leaved trees. We surveyed a chestnut tree grown in Yamakiya, which is located approximately

* Corresponding author.

E-mail address: sasaki.yoshito@jaea.go.jp (Y. Sasaki).

35 km northwest of the FDNPP. We measured the radiocesium concentration of the tree and that of the soluble ($<0.45 \mu\text{m}$) and particulate ($>0.45 \mu\text{m}$) fractions of the stemflow. Particulate fractions were identified through observation with a scanning electron microscope and an energy dispersive X-ray spectrometer.

2. Materials and methods

2.1. Sampling location

The study site is located in the forest of Yamakiya Sakashita, Kawamata Town, Date-gun, in the Fukushima Prefecture, approximately 35 km northwest of the FDNPP (Fig. 1). This site is a mixed forest mainly comprising *Quercus serrata* Murray (Konara), *Quercus crispula* Blume (Mizunara), and *Castanea crenata* Siebold et Zucc. (Japanese Chestnut), as well as some *Pinus densiflora* Sieb. et Zucc. (Japanese red pine) on the ridges and forest edges. The forest floor vegetation is partially covered by *Sasa nipponica* Makino et Shibata (Dwarf Bamboo). The thickness of the litter layer is approximately 1 cm, and the soil is classified as a brown forest soil.

2.2. Sampling

The samples of the Japanese Chestnut tree and the stemflow were collected from the same tree. The sampled chestnut tree had a height of 10.6 m, a diameter of 21.8 cm at breast height, and a

canopy projection area of 11.5 m^2 . Chestnut tree samples were obtained from branches of the canopy at a height of approximately 7 m in February 2014. The collected tree samples included a branch approximately 30 cm in length ($<5 \text{ mm}$) from the terminal and stem with a diameter of approximately 2 cm. The $\phi 2 \text{ cm}$ stem was separated between the wood and the bark. For use in measurements of radiocesium concentration in chestnut foliage, fallen leaves were collected immediately after defoliation in November 2013. The samples were dried to a constant weight at 90°C . The dried samples were placed in 80 ml capacity polystyrene V7 containers for measurement of the radiocesium concentration. Chestnut foliage for autoradiography was obtained using pruning scissors from the canopy at a height of 4 m in October 2013.

Stemflow was collected from September 2013 to July 2014, excluding the winter season from January to March 2014. The stemflow was collected using a stemflow collector shown in Appendix 1, which consisted of tubing (polyvinyl chloride, outer diameter 20 mm, inner diameter 15 mm) and was bound around the circumference of the tree trunk at 1.5 m above the ground. A plastic sheet was looped around the tubing, and drain tubing (polyvinyl chloride, outer diameter 20 mm, inner diameter 15 mm) was connected to a 70 l tank (polypropylene). The clearance between the tree trunk, the plastic sheet, and the tubing was filled with silicone rubber sealant. Stemflow that was blocked by bonding tubing around the trunk was collected into the tank through the drain tubing. In addition to the chestnut tree, stemflow was

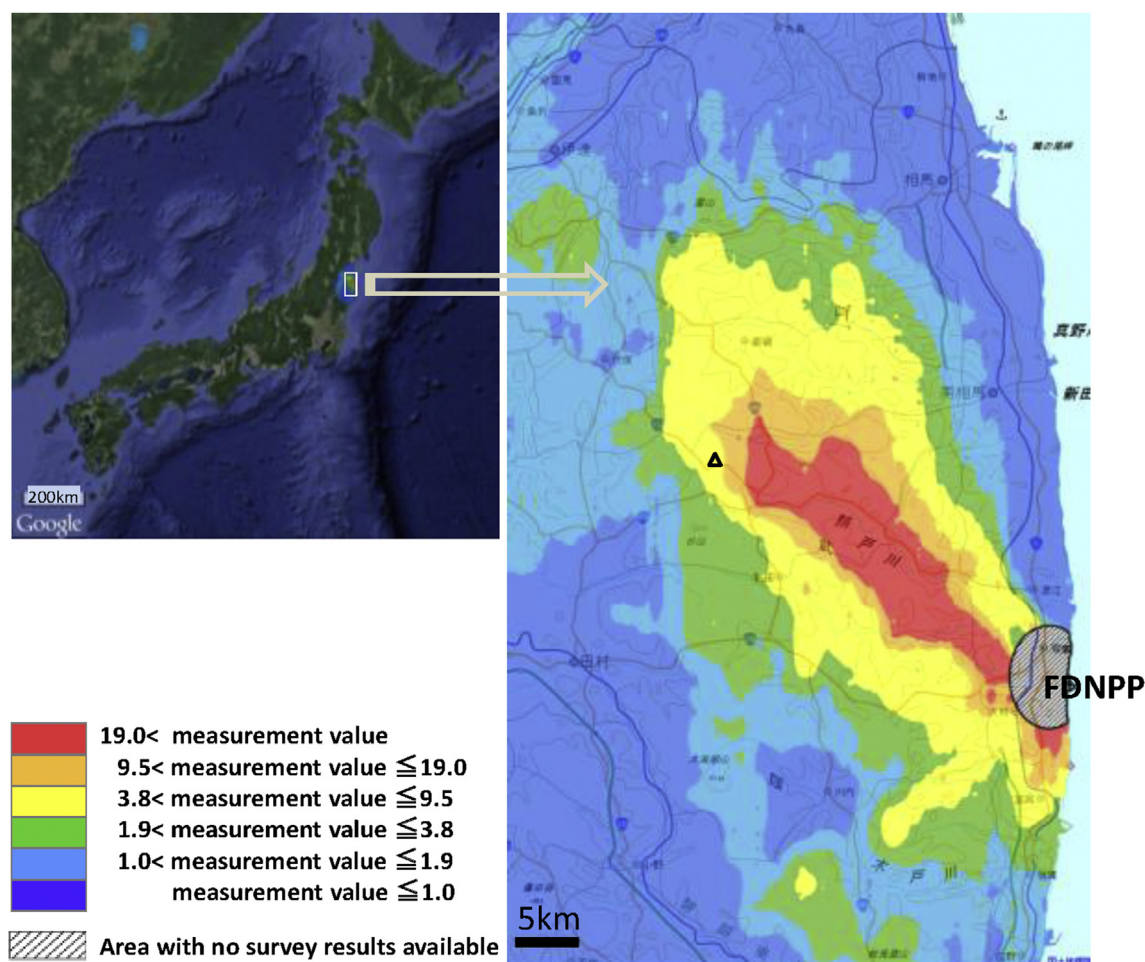


Fig. 1. Air dose rates ($\mu\text{Sv/h}$) at 1 m above the ground surface on April 29, 2011 (<http://ramap.jmc.or.jp/map/eng/map.html>) and the location of the sampling site in the Yamakiya area, Kawamata town, Fukushima Prefecture. The triangle indicates the sampling site. The GPS coordinates of the field site are $37^\circ35'17.7''\text{N}$ $140^\circ42'08.3''\text{E}$.

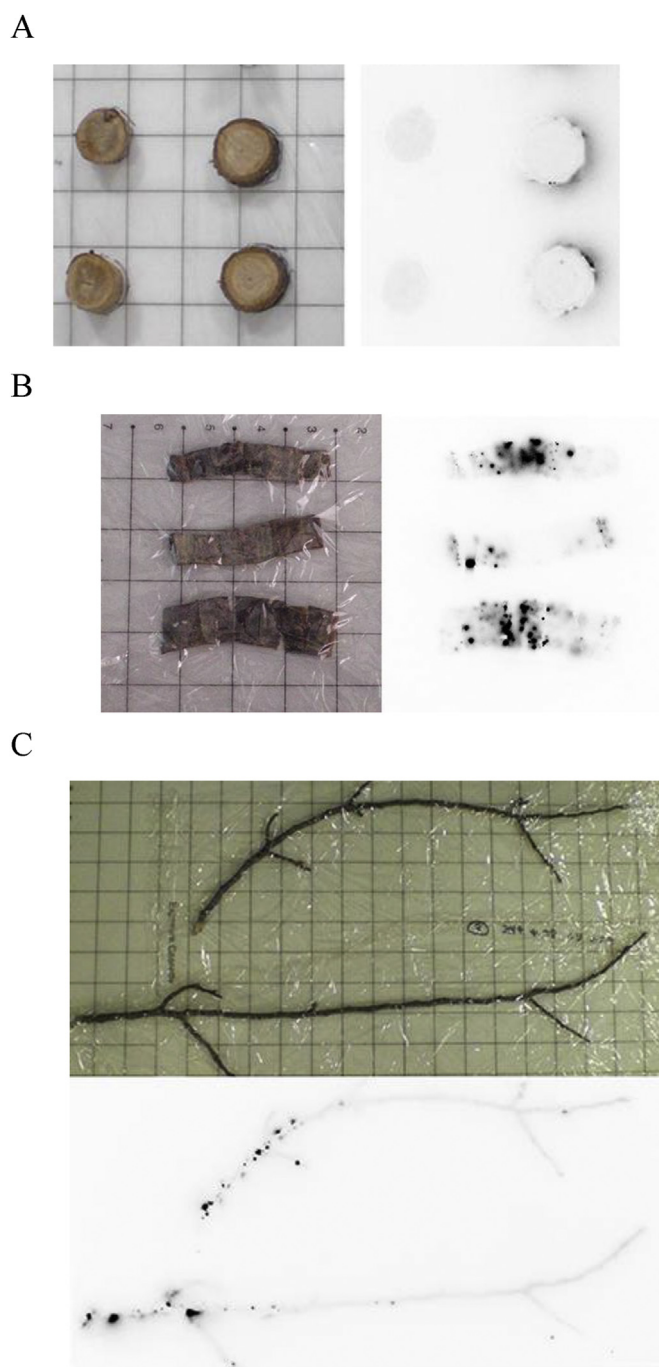


Fig. 2. Distribution of radioactivity in the sampled chestnut tree. A. Photograph of cross-section of $\phi 2$ cm stem (right) and $\phi 2$ cm stem without the bark (left) with corresponding autoradiographs. B. Photograph of the bark isolated from $\phi 2$ cm stem with corresponding autoradiographs. C. Photograph of $<\phi 5$ -mm stem with corresponding autoradiographs. The squares in the photographs have sides of 2 cm.

collected and analyzed from two *Q. serrata* from October 2013 to December 2013. The first sampled *Q. serrata* tree (tree no. 1) had a height of 9.09 m, a diameter of 11.1 cm at breast height, and a canopy projection area of 32.5 m². The second sampled *Q. serrata* tree (tree no. 2) had a height of 9.70 m, a diameter of 13.1 cm at breast height, and a canopy projection area of 38.8 m². The collected stemflow was filtered through a 47 mm diameter filter with a pore size of 0.45 μ m, namely the Durapore® PVDF Membrane Filter (HVLPO4700, Merck Millipore, Massachusetts, USA). After the

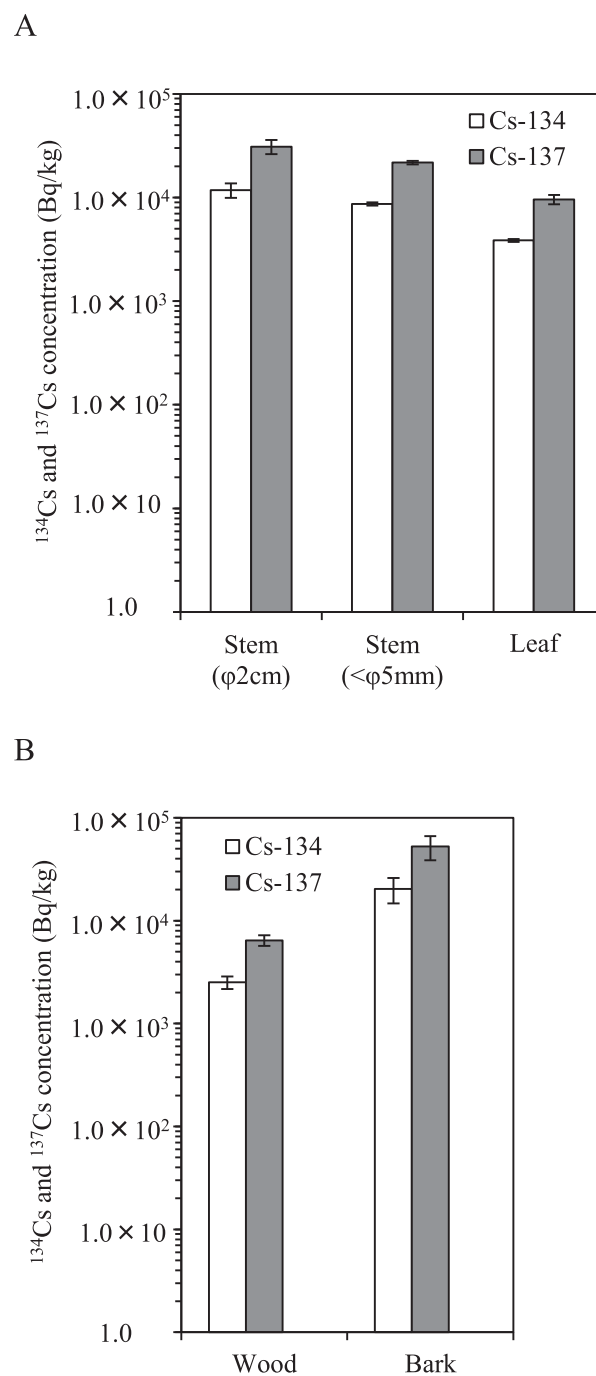


Fig. 3. Radiocesium concentrations in different parts of the chestnut tree. A. Radiocesium concentration of $\phi 2$ cm stems, $<\phi 5$ mm stems, and leaves. B. Radiocesium concentration of the wood and the bark in $\phi 2$ cm stems. The error bars represent the standard deviation of the sampling chestnut trees ($n = 3$).

filtration, stemflow samples were placed in a 500 ml plastic bottle to measure the radioactivity concentration. The sample residues on the membrane filter were dried to a constant weight at 90 °C and used for measuring the radioactivity concentration and distribution on the filter by autoradiography. Ultrafiltration was applied to the samples collected in October after filtration with the filter of pore size 0.45 μ m. Approximately 70 ml of the filtered water was ultrafiltered with a Vivaspin 20 MWCO (MWCO: molecular weight

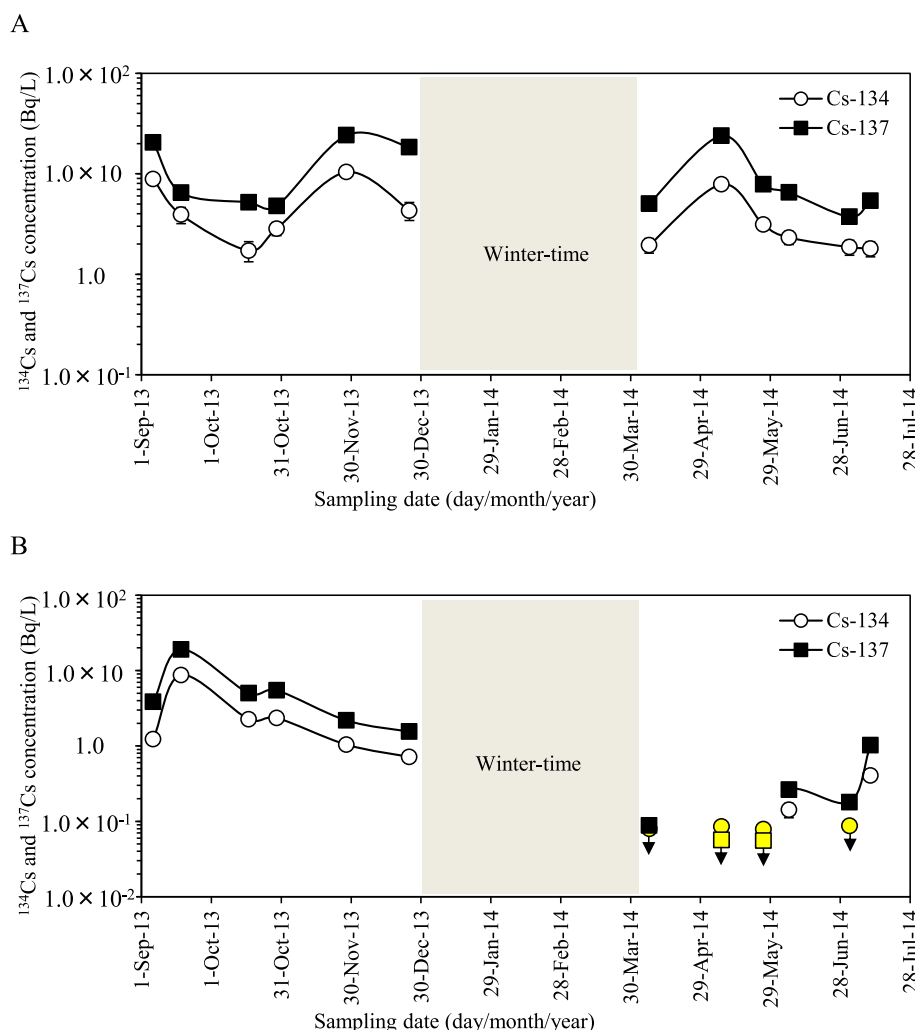


Fig. 4. Radiocesium concentration in stemflow through time. A. Dissolved fraction ($<0.45 \mu\text{m}$). B. Particulate fraction ($>0.45 \mu\text{m}$). The downward-pointing arrows with yellow markers indicate the detection limit. The error bars represent a counting error of 1σ . (For interpretation of the references to colour in this figure legend, the reader is referred to the web version of this article.)

cut-off) at 10 kDa (Da: daltons) and 100 kDa (Sartorius AG, Göttingen, Germany), respectively. After the ultrafiltration, stemflow samples were placed in 80 ml plastic containers (V7 containers) to measure the radioactivity concentration.

2.3. Measurements of the radiocesium concentration

Gamma-ray emissions at energies of 604 keV (^{134}Cs) and 661 keV (^{137}Cs) were measured using an n-type high-purity Ge-detector (GMX40P4-76 germanium detector, Seiko EG&G ORTEC, Tokyo, Japan) with a relative efficiency of 40%. For pulse-height analysis, a multichannel analyzer (MCA7600, Seiko EG&G ORTEC) was used in line with the spectrum analysis software (Gamma Studio, Seiko EG&G ORTEC). The efficiency calibration was conducted with a multiple gamma-ray emitting standard source (including 10 nuclides) packed in the same type of vessel (Eckert & Ziegler Isotope Products, California, USA) or in a plastic disc with the same active area ($\phi 42 \text{ mm}$) as the membrane filter (Eckert & Ziegler Nuclitec GmbH, Braunschweig, Germany). The decay of radiocesium was corrected for the time elapsed since sampling. The detection limits with a measurement time of 1200 s for ^{134}Cs and ^{137}Cs were $2.0 \times 10^2 \text{ Bq/kg}$ and $1.7 \times 10^2 \text{ Bq/kg}$, respectively, for a tree sample packed in a V-7 container. The detection limits with a

measurement time of 54,000 s for ^{134}Cs and ^{137}Cs were 1.7 Bq/L and 1.3 Bq/L, respectively, for measurements of stemflow packed in a V-7 container. The detection limits with a measurement time of 7200 s for ^{134}Cs and ^{137}Cs were 1.5 Bq/L and 1.2 Bq/L, respectively, for measuring the soluble fraction of stemflow packed in a 500 mL plastic bottle. The detection limits with a measurement time of 54,000 s for ^{134}Cs and ^{137}Cs were $1.0 \times 10^{-1} \text{ Bq/L}$ and $7.0 \times 10^{-2} \text{ Bq/L}$, respectively, for measuring the particulate fraction of the stemflow on membrane filters.

2.4. Measurements of pH and electrical conductivity

Measurements of the pH values and the electrical conductivity of the stemflow were obtained using a compact pH meter (B-712, Horiba, Kyoto, Japan) and a compact conductivity meter (B-771, Horiba).

2.5. Statistical analysis

The relationship between the ^{137}Cs concentration and the electrical conductivity in the stemflow was investigated using Pearson's correlation test. $P \leq 0.05$ was considered statistically significant.

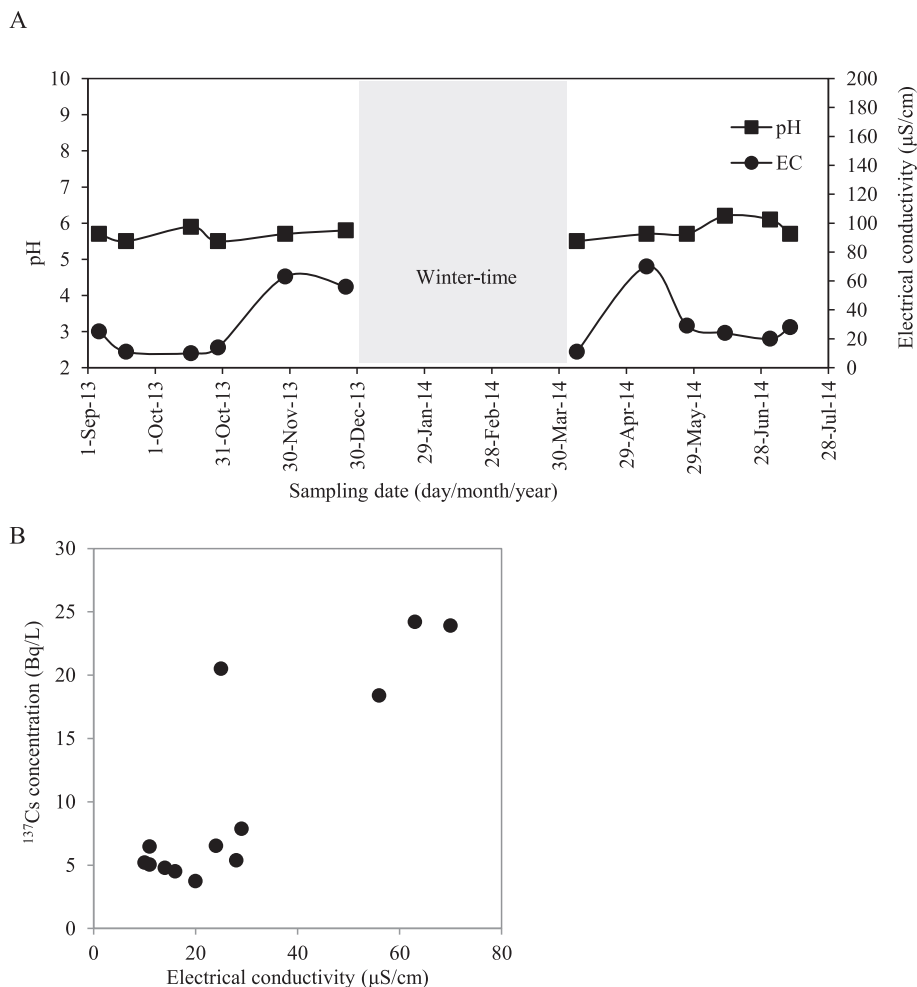


Fig. 5. A. Stemflow pH and electrical conductivity through time. B. Relation between stemflow ¹³⁷Cs concentration and electrical conductivity.

2.6. Autoradiography measurement

Plant parts (stem, bark, and foliage) and stemflow particles on a membrane filter were covered by polyvinylidene chloride thin film and polyethylene (0.04 mm), respectively. The samples were exposed for 4 days to the imaging plate BAS-IP, with 100-μm pixels (MS 2040, Fuji Film, Tokyo, Japan). The autoradiograph images were scanned using a laser scanner (Typhoon FLA7000, GE Healthcare, Little Chalfont, UK).

2.7. Observations of the particulate fraction of the stemflow

The stemflow was filtered through an isopore hydrophilic membrane with a pore size of 0.4 μm (HTTP02500, Merck Millipore). Scanning electron microscope (SEM) and energy dispersive X-ray spectrometer (EDS) observations of particles on the membrane filters were obtained using an Analytical SEM (JSM-6010LA, JEOL Ltd., Tokyo, Japan).

3. Results and discussion

3.1. Radiocesium distribution in the chestnut tree

Autoradiographs of the chestnut stem and bark are shown in Fig. 2. A heterogeneous radiocesium distribution was observed along the outer part of the stem with the bark in the cross-section

of the φ2 cm stem (Fig. 2A right). No clear images indicated that the radiocesium was distributed homogeneously in the woody portion of the cross-sections of the φ2 cm stem without the bark (Fig. 2A left). An autoradiograph of the bark peeled from the tree had spotty radiocesium distributions (Fig. 2B), which reflected the heterogeneous distribution in the outer cross-section of the tree (Fig. 2A right). In the <φ5-mm stems, radiocesium was homogeneously distributed in the stems from the top to approximately 20 cm in length (right side of the photograph of Fig. 2C), which were newly grown after the accident, whereas a heterogeneous and spotted radiocesium distribution was observed in the other parts. Sakamoto et al. (2013) and Nakanishi et al. (2013) also reported that a spotty deposition was observed on the surface of the plants that had grown at the time of the accident. The reasons for the non-uniformity and spotty deposition on the bark of the chestnut are not certain but we speculate that it is because of i) the deposition of radiocesium from one direction at the time of the FDNPP accident, ii) uneven leaching of the radiocesium and detachment of the bark after the accident.

The radiocesium concentrations of the φ2 cm stem, the <φ5-mm stem, and the leaves are shown in Fig. 3A. The radiocesium concentration was greatest in the φ2 cm stem, less in the <φ5-mm stem, and least in the leaves. The radiocesium concentrations of the stems separated into those from the bark and the wood were measured (Fig. 3B) and the concentration in the bark was approximately 10 times that in the wood. The φ2 cm stem had a relatively

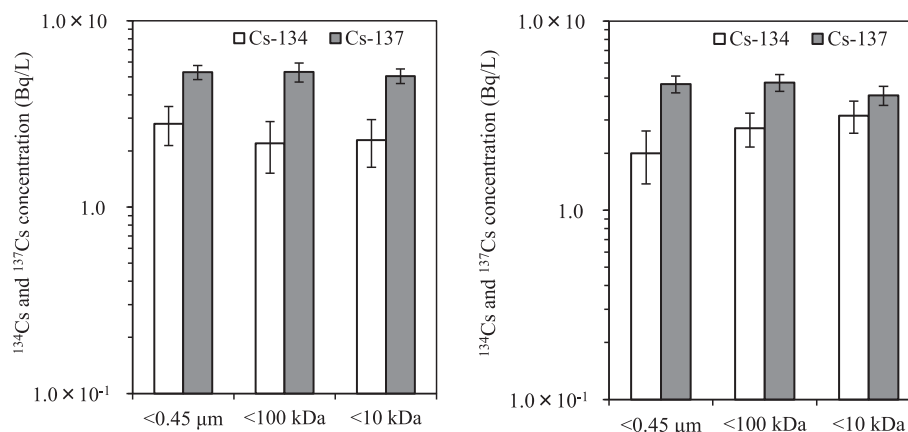


Fig. 6. The size distribution of ^{134}Cs and ^{137}Cs in the stem flow of the $<0.45\ \mu\text{m}$ fraction. Sampling date: left is October 17, 2013, right is October 29, 2013. The error bars represent a counting error of $1\ \sigma$.

high radiocesium concentration, probably because the stems were covered with old bark contaminated by the accident. The $<\phi 5\text{-mm}$ stems included stems contaminated by the accident and stems that only grew after the accident. This might be a reason the $<\phi 5\text{-mm}$ stems had lower concentrations than the $\phi 2\text{ mm}$ stems. Kanasashi et al. (2015) also reported that needles of Japanese cedar (*Cryptomeria japonica*) grown at time of the accident had higher radiocesium concentrations than those grown after the accident in planted forests in Fukushima. Newly grown leaves were the least contaminated, probably because of the lack of direct exposure to radiocesium from FDNPP.

3.2. Changes in the radiocesium concentration in the stemflow

The results of our monitoring of the temporal radiocesium concentration of the soluble fraction and the particulate fraction of the stemflow are shown in Fig. 4. The ^{137}Cs concentration of the soluble fraction varied between 3 and 24 Bq/L (average 1.05×10 Bq/L), and the radiocesium concentration did not show any decreasing trend (Fig. 4A). As for the particulate fractions, the ^{137}Cs concentration was between <0.06 and 10 Bq/L and tended to decrease gradually from 2013 to 2014 (Fig. 4B). We assumed that the elution of radiocesium from the bark to the stemflow was regulated by the difference in their concentrations of radiocesium. In our observations, the ^{137}Cs concentration ratio [bark that existed at the time of the accident (Bq/kg)/dissolved fraction of the

stemflow (Bq/L)] was approximately 10^3 . Besides bark samples, Tanaka et al. (2013) showed that the radiocesium concentration was strongly fixed in leaves through extraction experiments with pure water to remove the soluble fraction and the particle fraction of radiocesium from the contaminated leaves of *C. japonica*, *P. densiflora*, and *Q. serrata* (fallen leaves). In addition, Itoh et al. (2014) reported that radioactive particles attached to the leaves of evergreen plants were strongly attached to the surface and were not readily soluble in water. Further work is needed to elucidate whether there are differences in the elution mechanisms of radiocesium in the bark and leaves. However, a similar result was reported in a previous paper, specifically that radiocesium was detected in the soluble fraction and the particulate fraction of the stemflow of a beech tree growing in Germany, five years after the CNPP accident (Schimmack et al., 1993).

3.3. The soluble fraction of the stemflow

Measurements of the pH and the electrical conductivity of the stemflow are shown in Fig. 5A. The stemflow pH was almost constant with a value of approximately 5.8 during the measurement period. Plants are capable of buffering the acidity of rain, and K^+ , Mg^{2+} , and Ca^{2+} are leached from the plant in the buffering process (e.g., stemflow and throughfall) (Kohno et al., 2001; Parker, 1983; Pedersen et al., 1995). The collected stemflow was brown, indicating that organic matter from the tree was being leached. Organic

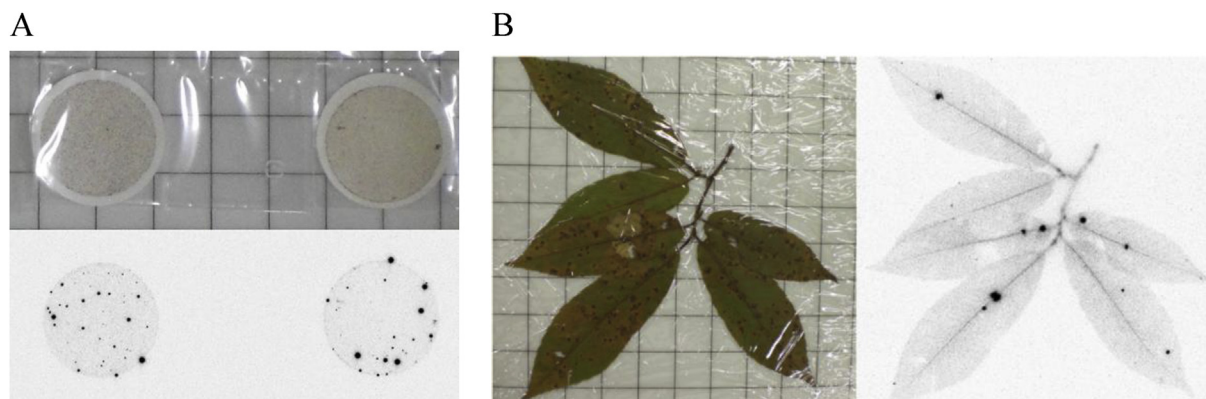


Fig. 7. A. Photographs of the particulate fraction ($>0.45\ \mu\text{m}$) with corresponding autoradiographs. Sampling date: left is October 17, 2013; right is October 29, 2013. B. Photograph of chestnut foliage with corresponding autoradiograph. Sampling date is October 29, 2013. The squares in the photographs have sides of 2 cm.

matter has also been reported to contribute to pH buffering (Fillion et al., 1998; Pedersen et al., 1995). The electrical conductivity of the stemflow varied between 10 and 70 $\mu\text{S}/\text{cm}$ in our study. There was a positive correlation between the radiocesium concentration and the electrical conductivity of the dissolved fraction of the stemflow as shown in Fig. 5B ($r = 0.865$, $P < 0.001$, $n = 13$). This result suggests that electrolytes and radiocesium in the stemflow are controlled by the same elution mechanism. We observed similar trends in the stemflow of Konara (*Q. serrata*), which belongs to the same family (*Fagaceae*) as the chestnut (Tree no. 1: $r = 0.994$, $P = 0.005$, $n = 4$; Tree no. 2: $r = 0.999$, $P < 0.001$, $n = 4$). Such a positive correlation between the radiocesium concentration and potassium concentration of the throughfall has also been reported for spruce and oak trees in Belgium, where contamination by the CNPP accident was observed (Ronneau et al., 1991). However, the dissolving mechanism from the bark to the stemflow is unclear for radiocesium, potassium (potassium and cesium are congeners), and other elements (e.g., calcium and magnesium). Moreover, note that the amount of stemflow, the shape and epiphytic angle of branches and leaves, and the smoothness of the bark may also be influenced (Crockford and Richardson, 2000; Levia and Frost, 2003). We need to study trees with different bark states and ages for further understanding.

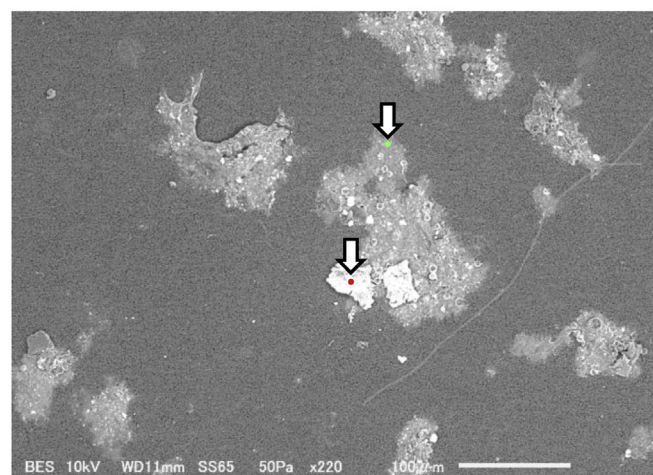
The chemical status of the stemflow in the $<0.45 \mu\text{m}$ fraction has been studied very little previously. The size distribution of the ^{134}Cs and ^{137}Cs particles in the stemflow of the $<0.45 \mu\text{m}$ fraction are shown in Fig. 6. The stemflow of the $<100 \text{ kDa}$ and the $<10 \text{ kDa}$ fraction had almost the same concentrations as those of the $<0.45 \mu\text{m}$ fraction. This result indicates that radiocesium in the $<0.45 \mu\text{m}$ fraction is present in an almost dissolved form, rather than as a complex form bound with organic matter. In the CNPP accident, ^{137}Cs in water extracts from organic layers of forest soils (in the Bavarian Alps, Germany) was mainly of an ionic form ($<500 \text{ Da}$) (Passeck et al., 1995). The radiocesium in the $<0.45 \mu\text{m}$ fraction of the river water also existed exclusively as a dissolved species rather than as a species adsorbed on suspended solids or in a complex form bound with organic matter (Matsunaga et al., 2004; Sakaguchi et al., 2015). The mobile form of radiocesium in water does not seem to exist as an organic complex, although the stemflow samples showed a brown color.

3.4. Particulate fraction of stemflow

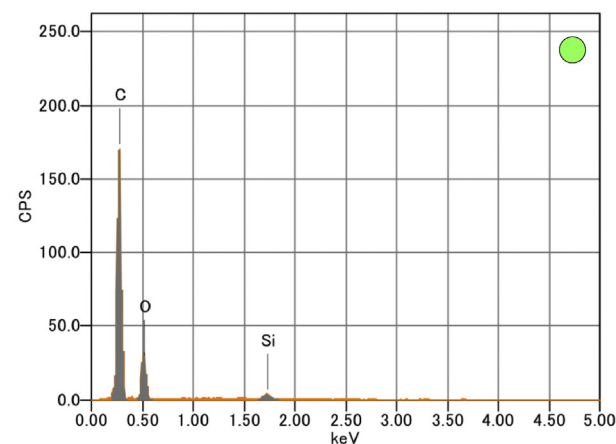
Autoradiographs of the particulate fraction of the stemflow are shown in Fig. 7A. Some of the particles in the stemflow contained a large amount of radiocesium. An autoradiograph of foliage collected in October 2013 (Fig. 7B) indicated that stem and leaf veins of the foliage were dotted with relatively strong radiocesium. Radiocesium detected as spots on the surface of the leaf might be part of the particulate fraction similar to that in the stemflow. A uniform distribution of radiocesium was observed in the leaves, with the exception of a few concentrated spots. This result suggests that radiocesium is supplied to the entire leaf through the veins along with water and nutrients.

SEM and EDS mappings of the particulate fractions of the stemflow of the Japanese chestnut are illustrated in Fig. 8. EDS point analysis reveals that the particulate fraction mostly comprises particles containing carbon, oxygen, and silica. These particles were assumed to be similar to detached organic matter; however, some of the particles contained carbon, oxygen, silica, aluminum, magnesium, and potassium. Some hardwood species could contain mineral inclusions of silica (Serdar and Demiray, 2012; IAWA Committee, 1989). However, because silica, aluminum, magnesium, and potassium are elements in clay minerals, cesium may be strongly adsorbed by clay minerals (Cremers et al., 1988; Valcke and

A



B



C

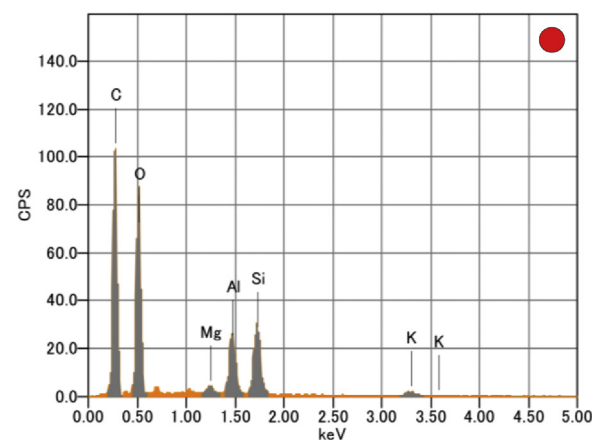


Fig. 8. Elemental analysis of particles in the particulate fraction ($>0.45 \mu\text{m}$) of the stemflow using SEM and EDS. A. SEM image of a particle from the particulate fraction on a membrane filter. The positions of the EDS point analysis are indicated by the arrowed red and green circles. B. EDS spectrum obtained by point analysis at the position indicated by the green circle. C. EDS spectrum obtained by point analysis at the position indicated by the red circle. Sampling date is October 29, 2013. (For interpretation of the references to colour in this figure legend, the reader is referred to the web version of this article.)

Cremers, 1994). Similar images of SEM and EDS were obtained for the particles in the stemflow of *Q. serrata* (data not shown). The inhomogeneous distribution of radiocesium in the particulate fraction of the stemflow seems to be related to the condition of the radiocesium distribution on the bark. Although particles containing radiocesium in the stemflow were detected in high numbers, they have not yet been identified. The depositional form of radiocesium on the bark is still unclear and further research is required.

4. Conclusion

The present investigation was conducted to elucidate the transition mechanism of radiocesium to the stemflow from the bark of deciduous broad-leaved trees contaminated with radiocesium by the FDNPP accident. We surveyed a chestnut tree grown in the Yamakiya area, Kawamata Town, which is located approximately 35 km northwest of the FDNPP. In the stem exposed to radiocesium from the accident, the concentration of the bark was approximately 10 times that inside the wood. The average ^{137}Cs concentration of the dissolved fraction ($<0.45\ \mu\text{m}$) of the stemflow was approximately 10 Bq/L. The ^{137}Cs concentration ratio [bark that was present at the time of the accident (Bq/kg)/dissolved fraction of stemflow (Bq/L)] was approximately 10^3 . Our result showing a positive relationship between the radiocesium concentration and the electrical conductivity of the dissolved fraction of the stemflow suggests that radiocesium and electrolytes have the same elution mechanism from the tree, although the dissolving mechanisms from the bark to the stemflow among radiocesium, potassium, and other elements has yet to be elucidated. The size fractionation analysis of the $<0.45\ \mu\text{m}$ fraction by ultrafiltration revealed that radiocesium was present as an almost dissolved species. Some of the particles in the particulate fraction ($>0.45\ \mu\text{m}$) of the stemflow were strongly adsorbed radiocesium. Further study of the transition mechanism from the bark to the stemflow for a greater variety of trees should help us further understand the behavior of radiocesium in the forest.

Acknowledgments

We express our sincere thanks to the anonymous reviewers who gave in valuable comments. We also thank the members of the Sector of Fukushima Research and Development, Fukushima Environmental Safety Center, JAEA and Dr. H. Sato (associate professor of Okayama University) for his advice. Moreover, we are grateful to Satoshi Maeda and Tsutomu Okazaki (Sasakino Analytical laboratory, Fukushima Radiation Measurement Group) for their technical help in measurement of radiocesium concentration.

Appendix A. Supplementary data

Supplementary data related to this article can be found at <http://dx.doi.org/10.1016/j.jenvrad.2015.12.001>.

References

- Adachi, K., Kajino, M., Zaizen, Y., Igarashi, Y., 2013. Emission of spherical cesium-bearing particles from an early stage of the Fukushima nuclear accident. *Sci. Rep.* 3, 2554. <http://dx.doi.org/10.1038/srep02554>.
- Chino, M., Nakayama, H., Nagai, H., Terada, H., Katata, G., Yamazawa, H., 2011. Preliminary estimation of release amounts of ^{131}I and ^{137}Cs accidentally

- discharged from the Fukushima Daiichi nuclear power plant into the atmosphere. *J. Nucl. Sci. Technol.* 48, 1129–1134.
- Chronological Scientific Tables (2014) ISBN10: 462108738X, ISBN13: 9784621087381.
- Cremers, A., Elsen, A., De Preter, P., Maes, A., 1988. Quantitative analysis of radiocesium retention in soils. *Nature* 335, 247–249.
- Crockford, R.H., Richardson, D.P., 2000. Partitioning of rainfall into throughfall, stemflow and interception: effect of forest type, ground cover and climate. *Hydrol. Process.* 14, 2903–2920.
- Fillion, N., Probst, A., Probst, J.L., 1998. Natural organic matter contribution to throughfall acidity in French forests. *Environ. Int.* 24, 547–558.
- IAWA Committee, 1989. IAWA list of microscopic features for hardwood identification. *n.s. IAWA Bull.* 10, 219–332.
- Itoh, S., Eguchi, T., Kato, N., Takahashi, S., 2014. Radioactive particles in soil, plant, and dust samples after the Fukushima nuclear accident. *Soil Sci. Plant Nutri.* 60, 540–550.
- Japan Meteorological Agency (2014) past 30 years (1981–2010).
- Kanasashi, T., Sugiura, Y., Takenaka, C., Hiji, N., Umemura, M., 2015. Radiocesium distribution in sugi (*Cryptomeria japonica*) in eastern Japan: translocation from needles to pollen. *J. Environ. Radioact.* 139, 398–406.
- Kaneyasu, N., Ohashi, H., Suzuki, F., Okuda, T., Ikemori, F., 2012. Sulfate aerosol as a potential transport medium of radiocesium from the Fukushima nuclear accident. *Environ. Sci. Technol.* 46, 5720–5726.
- Kato, H., Onda, Y., Gomi, T., 2012. Interception of the Fukushima reactor accident-derived ^{137}Cs , ^{134}Cs and ^{131}I by coniferous forest canopies. *Geophys. Res. Lett.* 39, L20403. <http://dx.doi.org/10.1029/2012GL052928>.
- Kohno, Y., Matsuki, R., Nomura, S., Mitsunari, K., Nakao, M., 2001. Neutralization of acid droplets on plant leaf surfaces. *Water Air Soil Pollut.* 13, 977–982.
- Levia, D.F., Frost, E.E., 2003. A review and evaluation of stemflow literature in the hydrologic and biogeochemical cycles of forested and agricultural ecosystems. *J. Hydrol.* 274, 1–29.
- Loffredo, N., Onda, Y., Kawamori, A., Kato, H., 2014. Modeling of leachable ^{137}Cs in throughfall and stemflow for Japanese forest canopies after Fukushima Daiichi nuclear power plant accident. *Sci. Total. Environ.* 493, 701–707.
- Mahara, Y., Ohta, T., Ogawa, H., Kumata, A., 2014. Atmospheric direct uptake and long-term fate of radiocesium in trees after the Fukushima nuclear accident. *Sci. Rep.* 4, 7121. <http://dx.doi.org/10.1038/srep07121>.
- Matsunaga, T., Nagao, S., Ueno, T., Takeda, S., Amano, H., Tkachenko, Y., 2004. Association of dissolved radionuclides released by the Chernobyl accident with colloidal materials in surface water. *Appl. Geochem.* 19, 1581–1599.
- Nakanishi, T.M., Kobayashi, N.I., Tanoi, K., 2013. Radioactive cesium deposition on rice, wheat, peach tree and soil after nuclear accident in Fukushima. *J. Radioanal. Nucl. Chem.* 296, 985–989.
- Parker, G.G., 1983. Throughfall and stemflow in the forest nutrient cycle. *Adv. Ecol. Res.* 13, 57–133.
- Passeck, U., Lindner, G., Zech, W., 1995. Distribution of ^{137}Cs in water leachates of forest humus. *J. Environ. Radioact.* 28, 223–238.
- Pedersen, L.B., Hansen, K., Bille-Hansen, J., Løber, M., Hovmand, M.F., 1995. Throughfall and canopy buffering in three sitka spruce stands in Denmark. *Water Air Soil Pollut.* 85, 1593–1598.
- Ronneau, C., Sombre, L., Myttenaere, C., Andre, P., Vanhouche, M., Cara, J., 1991. Radiocesium and potassium behaviour in forest trees. *J. Environ. Radioact.* 14, 259–268.
- Sakaguchi, A., Tanaka, K., Iwatani, H., Chiga, H., Fan, Q., Onda, Y., Takahashi, Y., 2015. Size distribution studies of ^{137}Cs in river water in the Abukuma Riverine system following the Fukushima Dai-ichi nuclear power plant accident. *J. Environ. Radioact.* 139, 379–389.
- Sakamoto, F., Ohnuki, T., Kozai, N., Yamasaki, S., Yoshida, Z., Nanba, K., 2013. Determination of local-area distribution and relocation of radioactive cesium in trees from Fukushima Daiichi nuclear power plant by autoradiography analysis. *Trans. At. Energy Soc. Jpn.* 12, 257–266 (in Japanese).
- Schimmack, W., Förster, H., Bunzl, K., Kreutzer, K., 1993. Deposition of radiocesium to the soil by stemflow, throughfall and leaf-fall from beech trees. *Radiat. Environ. Biophys.* 32, 137–150.
- Serdar, B., Demiray, H., 2012. Calcium oxalate crystal types in three oak species (*Quercus L.*) in Turkey. *Turk. J. Biol.* 36, 386–393.
- Tanaka, K., Iwatani, H., Sakaguchi, A., Takahashi, Y., Onda, Y., 2013. Local distribution of radioactivity in tree leaves contaminated by fallout of the radionuclides emitted from the Fukushima Daiichi nuclear power plant. *J. Radioanal. Nucl. Chem.* 295, 2007–2014.
- Teramag, M.T., Onda, Y., Kato, H., Gomi, T., 2014. The role of litterfall in transferring Fukushima-derived radiocesium to a coniferous forest floor. *Sci. Total. Environ.* 490, 435–439.
- Valcke, E., Cremers, A., 1994. Sorption-desorption dynamics of radiocesium in organic matter soils. *Sci. Total. Environ.* 157, 275–283.